RSC Advances

PAPER

Design, synthesis and antiproliferative evaluation of tetrahydro-β-carboline histone deacetylase inhibitors bearing an aliphatic chain linker†

Jing Shi,[ab] Jiayun Wang,[c] Xingjie Wang,[d] Chao Qu, [ID][d] Changchun Ye,[d] Xiuli Li,[b] Xin Chen [ID] *[c] and Zhengshui Xu [ID] *[a]

The use of histone deacetylase inhibitors (HDACis) is an effective approach for cancer treatment. In this work, a series of hydroxamic acid-based HDACis with a tetrahydro-β-carboline core and aliphatic linker have been designed and synthesized. The optimal compound **13d** potently inhibited HDAC1 and showed good antiproliferative activity against different tumor cell lines *in vitro*. Molecular docking of **13d** was conducted to rationalize the high binding affinity for HDAC1. Therefore, this work provides a new structure design for HDAC inhibitors and also offers a promising treatment for solid tumors.

1. Introduction

The regulation of histone modifications, including histone acetylation, methylation, or phosphorylation represent desirable drug targets due to aberrant epigenetic modulation in many cancers.[1,2] Histone deacetylases (HDACs), which control the acetylation levels of nuclear proteins and cytoplasmic proteins, have attracted wide attention for their crucial roles in the genesis and development of neoplasms.[3–5] The 11 classical zinc-dependent isoforms of mammalian HDAC are divided into four categories: class I (HDAC1, HDAC2, HDAC3, HDAC8), class IIa (HDAC4, 5, 7, 9), class IIb (HDAC6, 10), and class IV (HDAC11).[6,7] Class I HDACs, especially HDAC1, are important regulators of cell proliferation and a key oncology target.[8] Currently, many HDAC inhibitors are clinical, and five have been approved, namely, vorinostat,[9] belinostat,[10] panobinostat,[11] romidepsin[12] and chidamide.[13,14] The pharmacophore of HDAC inhibitors is well established: a capping motif occupying the outside of the protein's active pocket, a zinc-binding group (ZBG) chelating the catalytically active zinc ion, and a linker chain connecting the two parts (Fig. 1).[15–21] Hydroxamic acid is the most frequently used ZBG. Vorinostat (**1**), which was approved for the treatment of cutaneous T-cell lymphoma. Belinostat (**2**) gained U.S. Food and Drug Administration approval for the treatment of peripheral T-cell lymphoma. Panobinostat (**3**) was approved for the treatment of multiple myeloma. Selective HDAC6i ACY-1215 (**4**) was clinically evaluated for the treatment of multiple types of tumors.[22] It preferentially inhibited HDAC6 with an IC$_{50}$ of 4.7 nM, but also showed potent HDAC1 inhibition at 58 nM. However, most solid tumors have shown limited response to HDAC inhibitors, in contrast to the success with lymphoma in the clinic.[23] Hence, the development of either selective or pan-HDACis with better efficacy against solid tumors is of importance.

Tetrahydro-β-carboline (THβC, **5**) exists in a large number of natural compounds with different biological properties, such as antiviral, antimalarial, antithrombotic, antithrombotic, analgesic, anticancer and neurodegenerative activities.[24] Its semi-rigid structure (active indole ring and flexible piperidine motif) shows preferential affinities against different receptors and can be used as both an H-bond receptor and H-bond donor. This privileged scaffold also matches the characteristics of a capping group, which generally consists of hydrophobic and aromatic structures. Moreover, the THβC scaffold could be obtained through easy steps and is convenient for the construction of compound libraries. Hence, structural optimization on the THβC scaffold is a promising strategy for drug discovery.[25,26] In this paper, we attached a typical aliphatic linker and the ZBG hydroxamic acid present in multiple HDACis to this scaffold, and the chirality of the two chiral centers (C1 and C3) of the THβC derivatives were also adjusted through the introduction of various substituents (Fig. 2). Here, we report the synthesis, structure–activity relationship analysis and antiproliferative activity of these new molecules.

[a]Department of Thoracic Surgery, The Second Affiliated Hospital of Xi'an Jiaotong University, Xi'an, Shaanxi, 710004, China. E-mail: xuzhengshui@xjtu.edu.cn; Fax: +86-029-87679000

[b]Department of Respiratory and Endocrinology, The Second Affiliated Hospital of Xi'an Jiaotong University, Xi'an 710004, Shaanxi, China

[c]Shaanxi Key Labotory of Natural Products & Chemical Biology, College of Chemistry & Pharmacy, Northwest A&F University, Yangling 712100, China. E-mail: chenxin1888@nwsuaf.edu.cn; Fax: +86-029-87092335

[d]Department of General Surgery, The First Affiliated Hospital of Xi'an Jiaotong University, Xi'an, 710061, Shaanxi, China
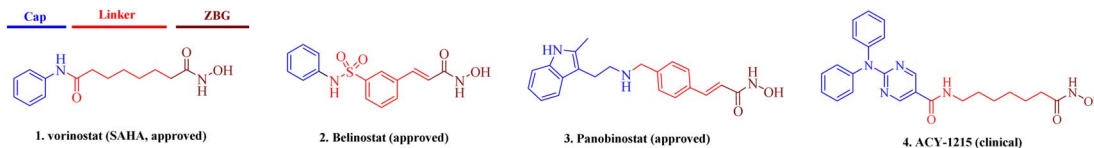
Fig. 1 Representative approved and clinical hydroxamic-acid-based HDAC inhibitors.
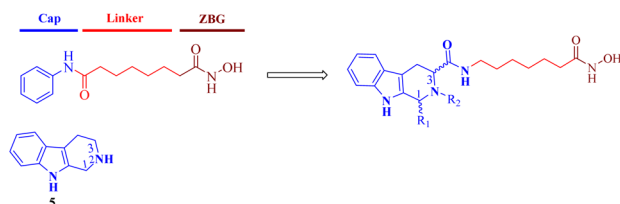

Fig. 2 Design of THβC-based HDAC inhibitors.

## 2. Chemistry

2.1 Chemistry

As outlined in Schemes 1 and 2, the key procedure for the synthesis of THβC derivatives was the application of the Pictet–Spengler cyclization from chiral tryptophan and aldehyde precursors according to our previous reports.[26,27] Under acidic conditions, the use of L-tryptophan (6) or D-tryptophan (10) with different aldehydes gave predominantly the desired thermodynamically stable *trans*-THβCs 7a–g or 11a–g. Alkylation of the N2 position with allyl bromide gave intermediates 8a–b using potassium carbonate as the base (Scheme 1). The building blocks 7a–g and 8a–b were then hydrolyzed and subsequently coupled with commercially available 6-amino-N-

hydroxyheptanamide or 7-amino-N-hydroxyhexanamide to provide the corresponding esters, which upon treatment with an aqueous $NH_2OH/NaOH$ solution yielded the targeted (1R,3S)-THβCs 9a–i. A similar chemical route was also used to prepare (1S,3R)-THβCs 13a–j in Scheme 2.

3. Results and discussion

3.1 HDAC1 activities and SAR study of the THβC derivatives

All the synthesized compounds were preliminarily evaluated for their inhibition rate (IR) against HDAC1 at 500 nM with pan-HDACi SAHA as reference. For compounds with an IR of over 80%, the IC_{50} values were further calculated. As shown in Table 1, the (1S,3R)-THβC analogues such as 13a (44.3%, IR) and 13f (91.4%, IR) were superior to the corresponding (1R,3S)-isomers such as 9a (31.8%, IR) and 9f (40.8%, IR). In comparison with 13b (49.2%, IR) and 13e (84.8%, IR; 53.6 nM, IC_{50}), compounds 13c (66%) and 13f (91.4%, 22.4 nM) with an aliphatic linker of six carbon atoms had better HDAC1 inhibition, indicating the importance of the length of the spacers separating the hydroxamic acid and THβC motifs. Structural optimization was also performed to explore the impact of different substituents on the C1 and N2 positions. C1-substituted THβCs 13i (4-chlorophenyl) and 13j (3,4-dimethoxyphenyl) showed IRs of
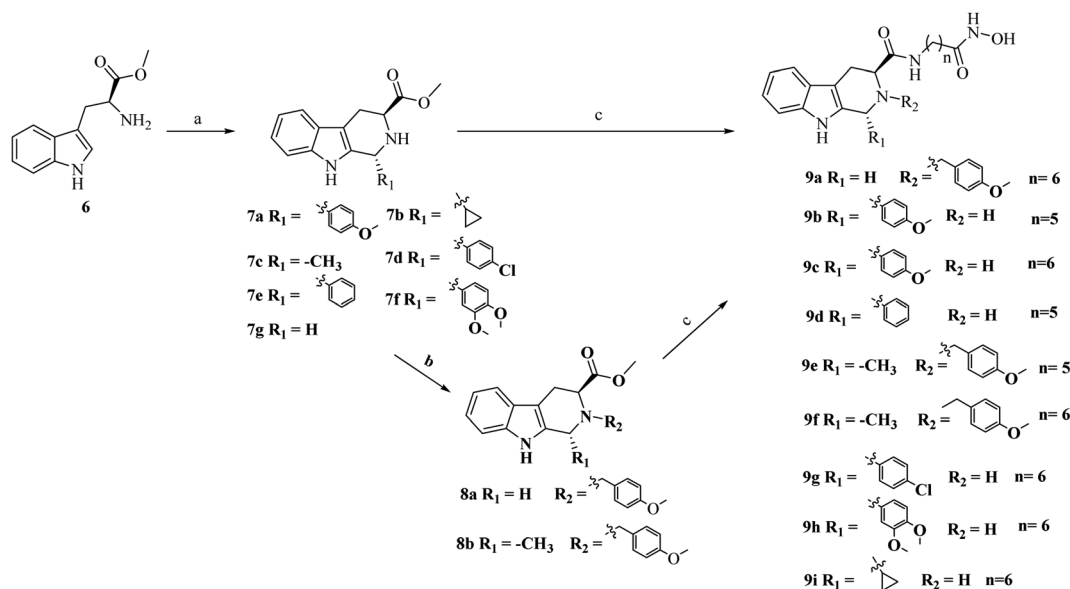
Scheme 1 Reagents and conditions: (a) isopropanol (i-PrOH), various aldehydes, reflux, overnight; (b) K_2CO_3, CH_3CN, 4-methoxybenzyl bromide, r.t., overnight; (c) (i) LiOH, MeOH : H_2O (V : V = 5 : 1), r.t., overnight; (ii) 2-(7-aza-1H-benzotriazole-1-yl)-1,1,3,3-tetramethyluronium hexafluorophosphate (HATU), N,N-diisopropylethylamine (DIPEA), N,N-dimethylformamide (DMF), 7-amino-N-hydroxyheptanamide or 6-amino-N-hydroxyhexanamide, 0 °C, 6 h; (iii) NH_2OH (aq), KOH, MeOH, 0 °C, 6 h.
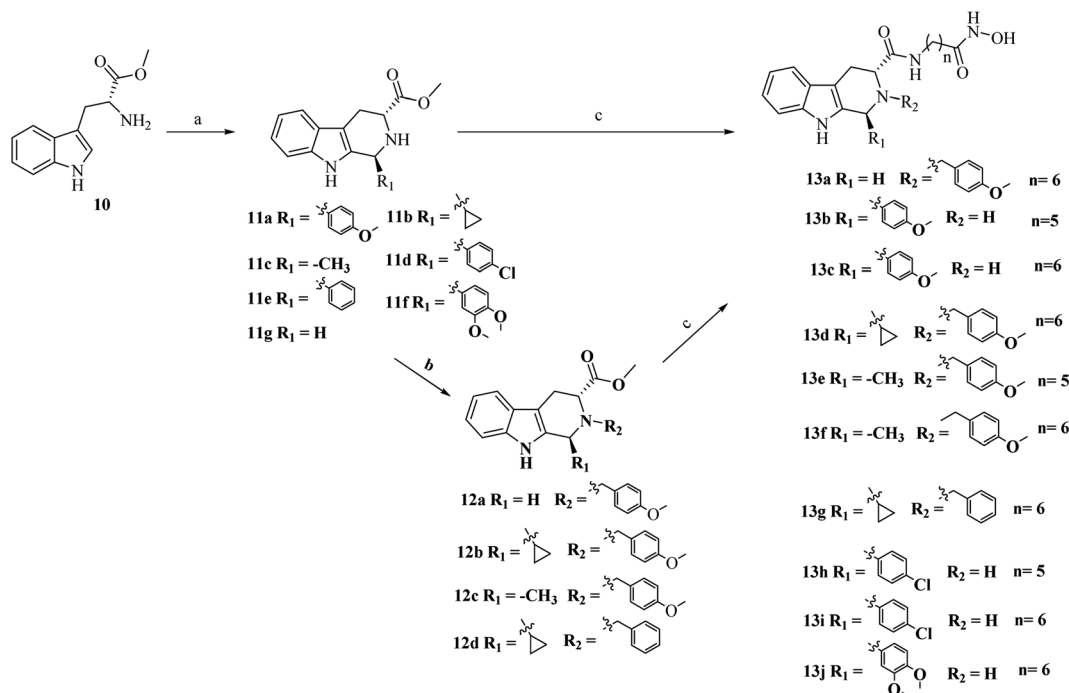
Scheme 2 Reagents and conditions: (a) i-PrOH, various aldehydes, reflux, overnight; (b) K_2CO_3, CH_3CN, benzyl bromide or 4-methoxybenzyl bromide, r.t., overnight; (c) (i) LiOH, MeOH : H_2O (V : V = 5 : 1), r.t.; (ii) HATU, DIPEA, DMF, 7-amino-N-hydroxyheptanamide or 6-amino-N-hydroxyhexanamide, 0 °C, 6 h; (iii) NH_2OH (aq), KOH, MeOH, 0 °C, 6 h.

66% and 72.5% for HDAC1, respectively. Compound **13c** with a 4-methoxyphenyl group showed a moderate IR of 81.6%, while the simple N2-substituted **13a**, lacking a chiral center, showed a weak IR of 44.3%. Interestingly, **13d–g** with simultaneous C1 and N2 functionalization showed distinctly improved potency with IRs between 84.8–99.2%. The IC_{50} test showed that the best compound **13d** inhibited HDAC1 with an IC_{50} of 8.73 nM. In comparison to the compounds with a hydrogen (**13a**) or methyl (**13f**) on the C1 position, the cyclopropyl-substituted THβC (**13d**) was a better choice, which indicated that the specific substituent on the C1 position maintained the active spatial conformation of total molecule.

13d was further tested against other classic HDAC isozymes. As shown in Table 2, **13d** inhibited HDAC2 and HDAC3 with

IC_{50} values of 23.5 nM and 32.1 nM, respectively. **13d** also potently inhibited HDAC6 with an IC_{50} of 4.5 nM. Additionally, weak inhibition of HDAC11 was observed. For HDAC4/5/7/8/9, **13d** showed no activity.

3.2 Molecular simulation

We docked the most potent compound **13d** into the crystal structure of human HDAC1 (PDB code: 5ICN) to probe the potential interaction between the molecule and target. As shown in Fig. 3A, **13d** was predicted to bind to Zn^{2+} with its hydroxamate group chelating in a bidentate manner. Additionally, a hydrogen bond interaction was formed between hydroxamic acid and Tyr303. Moreover, the aliphatic chain linker of **13d** occupied the narrow 11 Å hydrophobic tunnel and

Table 1 Initial evaluation of THβC derivatives against HDAC1 (percent inhibition at a concentration of 500 nM and IC_{50}, nM)[a]

Compound	Inhibition%	IC_{50}	Compound	Inhibition%	IC_{50}
9a	31.8%	—[b]	**13a**	44.3%	—
9b	23.2%	—	**13b**	49.2%	—
9c	41.3%	—	**13c**	81.6%	47.0 ± 1.25
9d	39.6%	—	**13d**	99.2%	8.73 ± 0.46
9e	58.1%	—	**13e**	84.8%	53.6 ± 2.50
9f	40.8%	—	**13f**	91.4%	22.4 ± 0.84
9g	65.4%	—	**13g**	98.2%	10.4 ± 0.65
9h	46.5%	—	**13h**	51.3%	—
9i	77.3%	—	**13i**	66.0%	—
SAHA	—	4.24 ± 0.23	**13j**	72.5%	—

[a] We ran experiments in duplicate, SD < 15%. Assays were performed by Reaction Biology Corporation (Malvern, PA, USA). [b] / to —: not tested.

Table 2 Complete characterization of **13d** using all 11 class I, II and IV HDAC enzymes (IC$_{50}$^{a}, nM)

Compound	13d	SAHA	Compound	13d	SAHA
HDAC1	8.73 ± 0.46	4.24 ± 0.23	HDAC6	4.50 ± 0.21	7.80 ± 0.38
HDAC2	23.5 ± 1.03	12.1 ± 0.92	HDAC7	>50 000	>50 000
HDAC3	32.1 ± 1.44	3.34 ± 0.17	HDAC8	>50 000	1033 ± 54.5
HDAC4	>50 000	>50 000	HDAC9	>50 000	>50 000
HDAC5	>50 000	>50 000	HDAC11	1800 ± 106	895 ± 34.7

^{a} IC$_{50}$ values for enzymatic inhibition of HDAC enzymes. We ran experiments in duplicate. Assays were performed by Reaction Biology Corporation (Malvern, PA, USA).
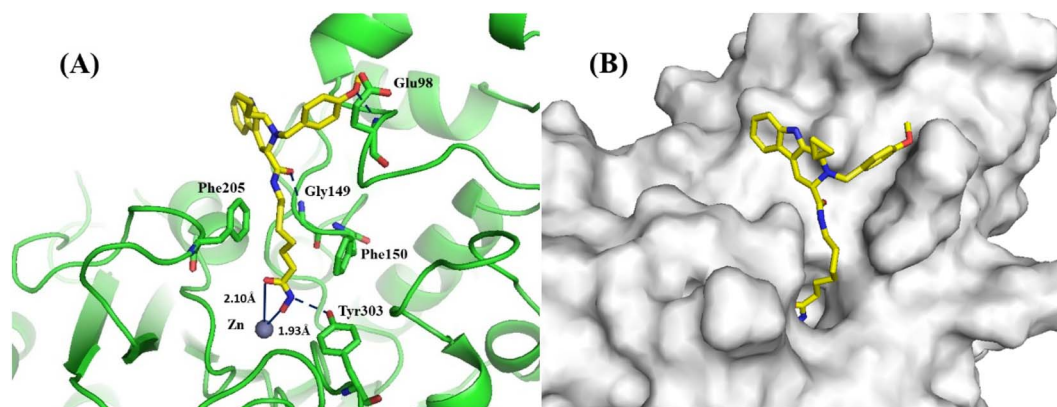

Fig. 3 (A) Binding model of **13d** (yellow) in the catalytic pocket of human HDAC1 (green cartoon). Key residues are labeled and shown as green sticks. Metal bonds and hydrogen bonds are labeled in dark blue. Zinc ions are shown in brown. (B) Surface map of **13d** with HDAC1. The deep active-site pocket is visualized with a transparent light-grey surface.

exhibited π-interactions with both Phe150 and Phe205. The amide at the entrance of this tunnel could generate a hydrogen bond with Gly149. As shown in Fig. 3B, the THβC group was positioned at the exposed hydrophobic surface of the enzyme. The cyclopropyl on the THβC scaffold extended into the upper region of capping part and avoided the cramped space below, indicating S-configuration of chiral C1 position was better adapted to the active pocket of HDAC1 protein. Besides, 4-methoxyphenyl ring on N2 was embedded in a branched pocket and formed an H-bond with Glu98. Such a binding mode matched well with the SAR of THβC derivatives in Table 1.

3.3 Antiproliferative evaluation

In view of the enzymatic potency, the preferred compounds **13d–g** and **13i** were screened against the colon cancer cell line HCT-116 and melanoma cell line SK-MEL-2. As shown in Table 3, all five THβCs showed potent antiproliferative activity with IC$_{50}$ values at the single-digit micromolar or sub-micromolar level. The foremost **13d** inhibited HCT116 and SK-MEL-2 with IC$_{50}$ values of 1.54 and 0.48 μM, outperforming the positive ACY-1215. Importantly, the potency of **13d** against SK-MEL-2 cells was obviously better than that of the approved compound SAHA. In addition, all four derivatives showed no influence on normal bone marrow cells HS-5.

Then, **13d** was submitted to NCI-60 for detailed examination of its antiproliferative activity against fifty-nine cancer cell lines. The cancer types in the NCI-60 program include leukemia, non-small-cell lung cancer, colon cancer, CNS cancer, melanoma, ovary cancer, renal cancer, prostate cancer and breast cancer. As shown in Table 4, **13d** displayed a broad-spectrum anticancer effect against leukemia and various solid tumors (>80% percent inhibition of 55 cell lines), especially colon cancer and melanoma.

Table 3 Antiproliferative effect of **13d–g** and **13i** against HCT-116 and SK-MEL-2 cell lines (IC$_{50}$^{a}, μM)

Compound	HCT116	SK-MEL-2	HS-5	Compound	HCT116	SK-MEL-2	HS-5
13d	1.54 ± 0.03	0.48 ± 0.01	>50	**13i**	7.55 ± 0.18	7.84 ± 0.26	>50
13e	8.34 ± 0.24	9.65 ± 0.46	>50	SAHA	1.30 ± 0.07	2.45 ± 0.08	—
13f	4.22 ± 0.12	5.70 ± 0.12	>50	ACY-1215	3.87 ± 0.11	4.50 ± 0.14	—
13g	3.20 ± 0.09	3.16 ± 0.08	>50				

^{a} IC$_{50}$ values are averages of three independent experiments, SD < 10%.

Table 4 Antiproliferative screening of **13d** against 59 cell lines (percent inhibition[a] at 10 μM)

Cancer type	Cell line	13d	Cancer type	Cell line	13d
Leukemia	CCRF-CEM	80.28		M14	82.4
	HL60	96.56		MDA-MB-435	100
	K-562	92.5		SK-MEL-2	100
	MOLT-4	87.83		SK-MEL-28	90.16
	RPMI-8226	84.29		SK-MEL-5	100
	SR	84.0		UACC-257	90.1
Non-small-cell lung cancer	A549/ATCC	82.73		UACC-62	100
	EKVX	83.23	Ovarian cancer	IGROV1	100
	HOP-62	86		OVCAR-3	96.77
	HOP-92	100		OVCAR-4	59.44
	NCI-H226	71.9		OVCAR-5	100
	NCI-H23	100		OVCAR-8	97.31
	NCI-H322M	90.5		NCI/ADR-RES	38.0
	NCI-H460	93.6		SK-OV-3	100
	NCI-H522	100	Renal cancer	786-0	82.65
Colon cancer	COLO 205	100		A498	100
	HCC-2998	100		ACHN	99.3
	HCT-116	97.9		CAKI-1	96
				SN12C	92.15
	HCT-15	91.15		TK-10	100
	HT29	93.7		UO-31	92.33
	KM12	87.5		PC-3	80.88
	SW-620	100	Prostate cancer	DU-145	90.64
CNS cancer	SF-268	85.46		MCF7	93.61
	SF-295	100	Breast cancer	MDA-MB-231/ATCC	100
	SF-539	97.13		HS 578T	100
	SNB-19	93.3		BT-549	74.54
	SNB-75	89.8		T-47D	100
	U251	100		MDA-MB-468	95.94
Melanoma	LOX IMVI	100			
	MALME-3M	98.55			

[a] Assays were performed by National Cancer Institute (NCI) at a single concentration (10 μM).

4. Conclusion

THβC, a natural privileged skeleton, has unique advantages for drug development. In this paper, nineteen THβC derivatives were obtained, several of which showed potent HDAC1 inhibition. In a cellular assay, five THβCs exhibited micromolar antiproliferative activity against the colon cancer cell line HCT-116 and melanoma cell line SK-MEL-2. Further screening of representative **13d** showed promising anti-proliferative activity against solid tumor cell lines such as colon, melanoma, and breast cancer. Currently, these THβCs are being further studied in our lab.

5. Experimental section

5.1 Chemistry

Unless otherwise noted, all reagents and solvents were obtained commercially, were of the highest commercial quality, and were used without further purification. All reactions were monitored using thin layer chromatography (TLC) on silica-gel-coated plates (Merck 60 F254), pre-coated silicone plates, and UV visualization. The crude product was purified using silica gel column chromatography using the standard technique (200−300 mesh, Qingdao Marine Chemical Ltd, PR China). All reported volumes are for separated products and were not optimized. The ^{1}H and ^{13}C nuclear magnetic resonance (NMR) spectra were recorded using a Bruker DRX-400 (^{1}H-NMR 400 MHz, ^{13}C-NMR 101 MHz) using TMS as an internal standard. Chemical shifts (δ) are expressed in parts per million (PPM), and coupling constants (J) are given in Hertz (Hz). The melting points of all products were determined using an x-4 instrument (Beijing Tech Instrument Co., Beijing, PR China) without calibration.

5.1.1 General procedure for the construction of 1,3-disubstituted THβC scaffolds 7a–g and 11a–g. Tryptophan methyl ester hydrochloride (1 equiv.) and the corresponding aldehyde (1.1 equiv.) were dissolved in isopropanol and cooled to 0 °C with an ice bath. The mixture was stirred at reflux overnight. After completion of the reaction as monitored using TLC, the reaction mixture was basified with aqueous NaHCO$_3$ and extracted with ethyl acetate. The organic layer was washed with water and brine, dried over Na$_2$SO$_4$, filtered, and evaporated under reduced pressure. Purification using flash chromatography (SiO$_2$; ethyl acetate/PE system) yielded first the cis isomer, followed by the trans isomer.

The chemical information for compounds **7a**, **7g** and **11a–g** can be found in ref. 25. The chemical information for compounds **7b–f** can be found in ref. 26.

5.1.2 General procedure for the preparation of N2-alkylated THβC intermediates 8a–b and 12a–d. To a stirred mixture of 1,3-disubstituted THβC (1 equiv.) prepared in Section 5.1.1 and potassium carbonate (1.3 equiv.) in acetonitrile were added various chlorides at 0 °C. After stirring at r.t. overnight, the reaction mixture was neutralized to pH 7. The reaction mixture was then diluted with saturated sodium chloride and extracted with ethyl acetate. The combined organic extracts were dried over anhydrous Na_2SO_4 and concentrated under reduced pressure. Purification by flash chromatography (SiO_2; ethyl acetate/PE system) yielded the desired compounds.

The chemical information for compounds **8a** and **12a–c** can be found in ref. 25. The chemical information for compound **8b** can be found in ref. 26.

5.1.2.1 Methyl (1S,3R)-2-benzyl-1-cyclopropyl-2,3,4,9-tetrahydro-1H-pyrido[3,4-b]indole-3-carboxylate (12d). White solid, 56.3% yield. ^{1}H NMR (400 MHz, DMSO-d$_6$) δ: 10.56 (s, 1H), 7.82–7.77 (m, 1H), 7.48 (d, J = 7.7 Hz, 1H), 7.42 (d, J = 7.4 Hz, 2H), 7.35–7.20 (m, 3H), 7.03 (t, J = 7.4 Hz, 1H), 6.99 (t, J = 7.4 Hz, 1H), 4.09 (d, J = 15.0 Hz, 1H), 3.75 (d, J = 15.0 Hz, 1H), 3.92 (t, J = 5.3 Hz, 1H), 3.58 (s, 3H), 3.21 (d, J = 9.6 Hz, 1H), 3.11 (dd, J = 15.6, 4.4 Hz, 1H), 2.85 (dd, J = 15.4, 5.8 Hz, 1H), 0.77 (m, 1H), 0.51 (m, 1H), 0.43 (m, 1H), 0.28 (m, 2H). ^{13}C NMR (101 MHz, DMSO-d$_6$) δ: 164.07, 143.18, 138.47, 136.15, 131.41, 131.18, 128.13, 127.01, 126.66, 120.73, 117.74, 111.03, 105.84, 59.52, 57.11, 51.02, 42.02, 18.93, 15.61, 3.72. $[\alpha]_D^{20}$ = 20.55 (0.05 mg mL^{-1}, MeOH). ESI-MS m/z: 361.5 [M + H]$^+$.

5.1.3 General procedure C: preparation of target compounds 9a–i and 13a–j. (i) To a mixed solution of methanol and water (V : V = 5 : 1) were added various esters (1 equiv.) and LiOH (2 equiv.). The mixture was stirred at r.t. overnight. After completion of the reaction as monitored using TLC, the mixture was concentrated under reduced pressure and diluted with excess water. After being neutralized with acetic acid, the formed precipitate was collected using filtration, washed with water, and dried *in vacuo*. The acids could be used directly for the next step. (ii) To a stirred mixture of the acid (1 equiv.) obtained from step (i), HATU (1.2 equiv.), and DIPEA (2 equiv.) in DMF was added the corresponding ester (1 equiv.) at 0 °C. After being stirred at r.t. for 6 h, saturated sodium chloride was added. The mixture was then extracted with EtOAc. The combined organic extracts were dried over anhydrous Na_2SO_4 and concentrated under reduced pressure. The product was obtained using chromatography on a silica gel column. (iii) To a solution of hydroxylamine hydrochloride (1.96 g, 28 mmol) in 20 mL of methanol, KOH (1.58 g, 28 mmol) was added and allowed to react at 40 °C for 10 min. The reaction mixture was cooled to 0 °C and filtered. The various esters obtained from step ii were added to the filtrate, followed by KOH, and allowed to react at r.t. overnight. The reaction mixture was extracted with EtOAc. The organic layer was washed with saturated NH$_4$Cl aqueous solution and brine, dried over Na$_2$SO$_4$, filtered, and concentrated. The target compound was obtained using chromatography on a silica gel column.

5.1.3.1 (S)-N-(7-(Hydroxyamino)-7-oxoheptyl)-2-(4-methoxybenzyl)-2,3,4,9-tetrahydro-1H-pyrido[3,4-b]indole-3-carboxamide

(9a). White solid, yield: 39.2%, m.p.: 102.1–105.3 °C. ^{1}H-NMR (400 MHz, DMSO-d$_6$) δ: 10.53 (s, 1H), 10.26 (s, 1H), 8.61 (d, J = 1.5 Hz, 1H), 7.92 (t, J = 5.8 Hz, 1H), 7.33 (d, J = 7.7 Hz, 1H), 7.25 (d, J = 8.6 Hz, 2H), 7.18 (d, J = 7.7 Hz, 1H), 6.94 (t, J = 7.5 Hz, 1H), 6.88 (t, J = 7.5 Hz, 1H), 6.84 (d, J = 8.6 Hz, 2H), 3.75 (d, J = 16.3 Hz, 1H), 3.68 (s, 3H), 3.63–3.48 (m, 4H), 3.13–3.04 (m, 1H), 3.02–2.89 (m, 2H), 2.77 (dd, J = 15.7, 5.3 Hz, 1H), 1.83 (t, J = 7.4 Hz, 2H), 1.45–1.32 (m, 4H), 1.24–1.07 (m, 4H). ^{13}C-NMR (101 MHz, DMSO-d$_6$) δ: 171.48, 169.14, 158.43, 135.90, 131.47, 130.70, 129.85, 126.89, 120.42, 118.31, 113.69, 110.86, 105.08, 61.04, 55.25, 55.07, 46.01, 38.43, 32.26, 29.18, 28.35, 26.19, 25.12, 20.54. $[\alpha]_D^{20}$ = −6.9 (0.9 mg mL^{-1}, MeOH). ESI-MS m/z: 479.6 [M + H]$^+$.

5.1.3.2 (1R,3S)-N-(6-(Hydroxyamino)-6-oxohexyl)-1-(4-methoxyphenyl)-2,3,4,9-tetrahydro-1H-pyrido[3,4-b]indole-3-carboxamide (9b). White solid, yield of 48.3%, m.p.: 141.4–143.7 °C. ^{1}H NMR (400 MHz, DMSO-d$_6$) δ: 10.71 (s, 1H), 10.34 (s, 1H), 8.68 (s, 1H), 7.83 (t, J = 5.5 Hz, 1H), 7.44 (d, J = 7.7 Hz, 1H), 7.25 (d, J = 7.8 Hz, 1H), 7.12 (d, J = 8.6 Hz, 2H), 7.03 (t, J = 7.5 Hz, 1H), 6.99–6.93 (m, 2H), 6.88 (d, J = 8.6 Hz, 2H), 5.17 (s, 1H), 3.72 (s, 3H), 3.44–3.40 (m, 1H), 3.04 (m, 2H), 2.94 (dd, J = 15.2, 4.6 Hz, 1H), 2.69 (dd, J = 15.2, 9.5 Hz, 2H), 1.93 (t, J = 7.3 Hz, 2H), 1.52–1.43 (m, 2H), 1.44–1.35 (m, 2H), 1.24–1.18 (m, 2H). ^{13}C NMR (101 MHz, DMSO-d$_6$) δ: 172.57, 169.09, 158.39, 136.05, 129.42, 126.71, 120.77, 118.29, 117.62, 113.46, 111.00, 107.77, 55.11, 53.34, 51.69, 38.35, 32.23, 28.86, 26.04, 24.89. $[\alpha]_D^{20}$ = −12.14 (0.07 g/100 mL, MeOH). ESI-MS m/z: 451.5 [M + H]$^+$.

5.1.3.3 (1R,3S)-N-(7-(Hydroxyamino)-7-oxoheptyl)-1-(4-methoxyphenyl)-2,3,4,9-tetrahydro-1H-pyrido[3,4-b]indole-3-carboxamide (9c). Yellow solid, yield: 42.7%, m.p. 125.2–127.1 °C. ^{1}H NMR (400 MHz, DMSO-d$_6$) δ: 10.71 (s, 1H), 10.34 (s, 1H), 8.67 (s, 1H), 7.82 (t, J = 5.6 Hz, 1H), 7.44 (d, J = 7.7 Hz, 1H), 7.25 (d, J = 7.7 Hz, 1H), 7.13 (d, J = 8.6 Hz, 2H), 7.03 (t, J = 7.5 Hz, 1H), 6.96 (t, J = 7.5 Hz, 1H), 6.88 (d, J = 8.6 Hz, 2H), 5.17 (s, 1H), 3.72 (s, 3H), 3.41 (dd, J = 9.5, 4.6 Hz, 1H), 3.07–3.03 (q, J = 6.6 Hz, 2H), 2.94 (dd, J = 15.2, 4.6 Hz, 1H), 2.70 (dd, J = 15.2, 9.5 Hz, 1H), 1.93 (t, J = 7.3 Hz, 2H), 1.52–1.44 (m, 2H), 1.43–1.36 (m, 2H), 1.27–1.21 (m, 4H). ^{13}C NMR (101 MHz, DMSO-d$_6$) δ: 172.59, 169.15, 158.40, 136.05, 135.00, 134.77, 129.42, 126.73, 120.78, 118.30, 117.62, 113.46, 111.01, 107.78, 55.11, 54.94, 53.33, 51.71, 38.39, 32.26, 29.01, 28.32, 26.14, 25.16, 25.11. $[\alpha]_D^{20}$ = −13.2 (1 mg mL^{-1}, MeOH). ESI-MS m/z: 479.6 [M + H]$^+$.

5.1.3.4 (1R,3S)-N-(6-(Hydroxyamino)-6-oxohexyl)-1-phenyl-2,3,4,9-tetrahydro-1H-pyrido[3,4-b]indole-3-carboxamide (9d). Yellow solid, yield of 55.3%, m.p. 133.1–134.7 °C. ^{1}H NMR (400 MHz, DMSO-d$_6$) δ: 10.74 (s, 1H), 10.34 (s, 1H), 8.67 (s, 1H), 7.84 (t, J = 5.6 Hz, 1H), 7.45 (d, J = 7.7 Hz, 1H), 7.35–7.28 (m, 2H), 7.28–7.19 (m, 4H), 7.04 (t, J = 7.4 Hz, 1H), 6.97 (t, J = 7.4 Hz, 1H), 5.22 (s, 1H), 3.44–3.40 (m, 1H), 3.04 (q, J = 6.7 Hz, 2H), 2.95 (dd, J = 15.2, 4.6 Hz, 1H), 2.70 (dd, J = 15.2, 8.1 Hz, 2H), 1.95–1.89 (m, 2H), 1.55–1.34 (m, 4H), 1.29–1.17 (m, 2H). ^{13}C NMR (101 MHz, DMSO-d$_6$) δ: 172.59, 169.11, 143.02, 136.08, 134.42, 128.33, 128.12, 127.08, 126.71, 120.84, 118.34, 117.67, 111.04, 107.92, 53.90, 51.79, 38.36, 32.23, 28.87, 26.04, 25.25, 24.90. $[\alpha]_D^{20}$ = −40.5 (1 mg mL^{-1}, MeOH). ESI-MS m/z: 421.5 [M + H]$^+$.

5.1.3.5 (1R,3S)-N-(6-(Hydroxyamino)-6-oxohexyl)-2-(4-methoxybenzyl)-1-methyl-2,3,4,9-tetrahydro-1H-pyrido[3,4-b]indole-3-carboxamide (9e). Yellow solid, yield of 50.2%, m.p. 128.2–130.2 °C. ^{1}H NMR (400 MHz, DMSO-d$_6$) δ: 10.63 (s, 1H), 10.30 (s, 1H), 8.64 (s, 1H), 7.86 (t, J = 5.8 Hz, 1H), 7.43 (d, J = 7.9 Hz, 1H), 7.32 (d, J = 8.5 Hz, 2H), 7.25 (d, J = 7.9 Hz, 1H), 7.02 (t, J = 7.1 Hz, 1H), 6.96 (t, J = 7.1 Hz, 1H), 6.88 (d, J = 8.5 Hz, 2H), 3.87 (dd, J = 10.5, 4.8 Hz, 1H), 3.82–3.75 (m, 1H), 3.74 (s, 3H), 3.59 (d, J = 13.9 Hz, 1H), 3.38 (d, J = 14.3 Hz, 1H), 3.31–3.22 (m, 1H), 3.09–2.95 (m, 1H), 2.90–2.83 (m, 1H), 2.80–2.74 (m, 1H), 2.69 (s, 2H), 1.86 (t, J = 7.4 Hz, 2H), 1.48–1.35 (m, 6H), 1.29–1.14 (m, 3H). ^{13}C NMR (101 MHz, DMSO-d$_6$) δ: 171.65, 169.01, 158.25, 136.13, 136.00, 131.15, 129.15, 126.84, 120.49, 118.28, 117.64, 113.69, 110.82, 105.25, 56.25, 55.01, 51.07, 50.28, 38.34, 32.16, 29.09, 26.00, 24.84, 20.74, 18.76. $[\alpha]_D^{20}$ = 9.72 (1 mg mL^{-1}, MeOH). ESI-MS m/z: 479.6 [M + H]$^+$.

5.1.3.6 (1R,3S)-N-(7-(Hydroxyamino)-7-oxoheptyl)-2-(4-methoxybenzyl)-1-methyl-2,3,4,9-tetrahydro-1H-pyrido[3,4-b]indole-3-carboxamide (9f). White solid, yield of 27.5%, m.p.: 158.2–159.3 °C. ^{1}H NMR (400 MHz, DMSO-d$_6$) δ: 10.63 (s, 1H), 10.30 (s, 1H), 8.64 (s, 1H), 7.85 (t, J = 5.9 Hz, 1H), 7.43 (d, J = 7.6 Hz, 1H), 7.32 (d, J = 8.5 Hz, 2H), 7.25 (d, J = 7.9 Hz, 1H), 7.02 (t, J = 7.3 Hz, 1H), 6.96 (t, J = 7.3 Hz, 1H), 6.88 (d, J = 8.5 Hz, 2H), 3.87 (dd, J = 10.1, 4.9 Hz, 1H), 3.79 (d, J = 6.8 Hz, 1H), 3.75 (s, 1H), 3.58 (d, J = 14.0 Hz, 1H), 3.29 (m, 1H), 3.01 (m, 1H), 2.88 (dd, J = 16.0, 10.1 Hz, 1H), 2.76 (dd, J = 16.0, 4.9 Hz, 1H), 1.87 (t, J = 7.4 Hz, 2H), 1.45–1.31 (m, 4H), 1.26–1.09 (m, 4H). ^{13}C NMR (101 MHz, DMSO-d$_6$) δ: 171.68, 169.09, 158.27, 136.15, 136.02, 131.15, 129.13, 126.85, 120.52, 118.31, 117.66, 113.70, 110.84, 105.27, 56.28, 55.04, 51.09, 50.33, 38.42, 32.22, 29.27, 28.35, 26.12, 25.05, 20.78, 18.78. $[\alpha]_D^{20}$ = 11.3 (1 mg mL^{-1}, MeOH). ESI-MS m/z: 493.6 [M + H]$^+$.

5.1.3.7 (1R,3S)-1-(4-Chlorophenyl)-N-(7-(hydroxyamino)-7-oxoheptyl)-2,3,4,9-tetrahydro-1H-pyrido[3,4-b]indole-3-carboxamide (9g). White solid, yield of 62.9%, m.p.: 135.2–136.2 °C. ^{1}H NMR (400 MHz, DMSO-d$_6$) δ 10.76 (s, 1H), 10.34 (s, 1H), 8.67 (s, 1H), 7.84 (t, J = 5.6 Hz, 1H), 7.45 (d, J = 7.6 Hz, 1H), 7.38 (d, J = 8.4 Hz, 2H), 7.29–7.18 (m, 3H), 7.05 (t, J = 7.4 Hz, 1H), 6.97 (t, J = 7.4 Hz, 1H), 5.22 (s, 1H), 3.05 (q, J = 6.6 Hz, 2H), 2.92 (dd, J = 15.3, 4.7 Hz, 1H), 2.71 (dd, J = 15.3, 9.6 Hz, 1H), 1.93 (t, J = 7.3 Hz, 2H), 1.54–1.42 (m, 2H), 1.42–1.32 (m, 2H), 1.30–1.17 (m, 4H). ^{13}C NMR (101 MHz, DMSO-d$_6$) δ: 172.46, 169.13, 142.03, 136.06, 133.97, 131.63, 130.14, 128.03, 126.68, 120.95, 118.41, 117.72, 111.07, 108.03, 53.16, 51.77, 38.40, 32.26, 28.99, 28.32, 26.14, 25.10. $[\alpha]_D^{20}$ = −8.00 (1 mg mL^{-1}, MeOH). ESI-MS m/z: 470 [M + H]$^+$.

5.1.3.8 (1R,3S)-1-(3,4-Dimethoxyphenyl)-N-(7-(hydroxyamino)-7-oxoheptyl)-2,3,4,9-tetrahydro-1H-pyrido[3,4-b]indole-3-carboxamide (9h). White solid, 45.4% yield, m.p.: 145.1–146.7 °C. ^{1}H NMR (400 MHz, DMSO-d$_6$) δ: 10.72 (s, 1H), 10.35 (s, 1H), 8.68 (s, 1H), 7.87 (t, J = 5.4 Hz, 1H), 7.44 (d, J = 7.6 Hz, 1H), 7.26 (d, J = 7.9 Hz, 1H), 7.07–7.00 (m, 2H), 6.96 (t, J = 7.4 Hz, 1H), 6.85 (d, J = 8.3 Hz, 1H), 6.58 (d, J = 8.2 Hz, 1H), 5.17 (s, 1H), 3.73 (s, 3H), 3.71 (s, 3H), 3.45 (dd, J = 9.4, 4.8 Hz, 2H), 3.10–3.03 (m, 2H), 2.94 (dd, J = 15.1, 4.8 Hz, 1H), 2.72 (dd, J = 15.1, 9.4 Hz, 1H), 1.93 (t, J = 7.3 Hz, 2H), 1.50–1.37 (m, 4H), 1.26–1.23 (m,

4H). ^{13}C NMR (101 MHz, DMSO-d$_6$) δ: 172.64, 169.20, 148.69, 148.07, 136.09, 135.37, 134.77, 126.73, 120.83, 120.25, 118.34, 117.68, 112.32, 111.25, 111.05, 107.75, 55.61, 55.55, 53.69, 51.92, 38.42, 32.29, 29.07, 28.37, 26.18, 25.14. $[\alpha]_D^{20}$ = −15.2 (1 mg mL^{-1}, MeOH). ESI-MS m/z: 495.6 [M + H]$^+$.

5.1.3.9 (1R,3S)-1-Cyclopropyl-N-(7-(hydroxyamino)-7-oxoheptyl)-2,3,4,9-tetrahydro-1H-pyrido[3,4-b]indole-3-carboxamide (9i). White solid, yield of 36.2%, m.p.: 135.1–135.8 °C. ^{1}H NMR (400 MHz, DMSO-d$_6$) δ: 10.55 (s, 1H), 10.37 (s, 1H), 8.71 (s, 1H), 7.87 (t, J = 5.4 Hz, 1H), 7.41–7.32 (m, 2H), 7.03 (t, J = 7.5 Hz, 1H), 6.94 (t, J = 7.5 Hz, 1H), 3.38–3.36 (m, 1H), 3.27 (d, J = 8.8 Hz, 1H), 3.12 (q, J = 6.6 Hz, 2H), 2.89 (dd, J = 14.7, 3.2 Hz, 1H), 2.65–2.53 (m, 1H), 1.95 (t, J = 7.3 Hz, 2H), 1.56–1.38 (m, 4H), 1.35–1.18 (m, 4H), 0.98 (m, 1H), 0.75–0.57 (m, 2H), 0.55–0.35 (m, 2H). ^{13}C NMR (101 MHz, DMSO-d$_6$) δ: 172.47, 169.22, 136.47, 136.19, 126.75, 120.63, 118.41, 117.48, 111.37, 106.60, 57.72, 57.32, 38.46, 32.30, 29.11, 28.38, 26.20, 25.87, 25.15, 15.48, 3.31, 2.23. $[\alpha]_D^{20}$ = −16.9 (0.75 mg mL^{-1}, MeOH). ESI-MS m/z: 399.5 [M + H]$^+$.

5.1.3.10 (R)-N-(7-(Hydroxyamino)-7-oxoheptyl)-2-(4-methoxybenzyl)-2,3,4,9-tetrahydro-1H-pyrido[3,4-b]indole-3-carboxamide (13a). White solid, yield of 71.2%, m.p.: 139.8–141.8 °C. ^{1}H-NMR (400 MHz, DMSO-d$_6$) δ: 10.60 (s, 1H), 10.32 (d, J = 1.8 Hz, 1H), 8.66 (d, J = 1.8 Hz, 1H), 7.98 (t, J = 5.9 Hz, 1H), 7.39 (d, J = 7.6 Hz, 1H), 7.35–7.27 (m, 2H), 7.28–7.20 (m, 1H), 7.06–6.86 (m, 4H), 3.82 (d, J = 16.1 Hz, 1H), 3.74 (s, 3H), 3.72–3.62 (m, 3H), 3.64–3.54 (m, 3H), 3.17 (dq, J = 13.3, 6.8 Hz, 1H), 3.11–2.95 (m, 2H), 2.84 (dd, J = 15.7, 5.6 Hz, 1H), 1.90 (t, J = 7.4 Hz, 2H), 1.42 (q, J = 7.0 Hz, 5H), 1.22 (d, J = 8.3 Hz, 6H). ^{13}C-NMR (101 MHz, DMSO-d$_6$) δ: 171.93, 169.59, 158.88, 136.35, 131.91, 131.14, 130.30, 127.34, 120.87, 118.76, 117.85, 114.14, 111.30, 105.53, 61.48, 55.69, 55.51, 46.45, 39.63, 38.87, 32.69, 29.62, 28.79, 26.62, 25.56, 20.98. $[\alpha]_D^{20}$ = 21.87 (0.065 g/100 mL, MeOH). ESI-MS m/z: 479.6 [M + H]$^+$.

5.1.3.11 (1S,3R)-N-(6-(Hydroxyamino)-6-oxohexyl)-1-(4-methoxyphenyl)-2,3,4,9-tetrahydro-1H-pyrido[3,4-b]indole-3-carboxamide (13b). White solid, yield of 55.8%, m.p.: 101.3–103.7 °C. ^{1}H NMR (400 MHz, DMSO-d$_6$) δ: 10.71 (s, 1H), 10.34 (s, 1H), 8.67 (s, 1H), 7.82 (t, J = 5.6 Hz, 1H), 7.44 (d, J = 7.7 Hz, 1H), 7.25 (d, J = 7.7 Hz, 1H), 7.13 (d, J = 8.7 Hz, 2H), 7.03 (t, J = 7.1 Hz, 1H), 6.96 (t, J = 7.1 Hz, 1H), 6.88 (d, J = 8.7 Hz, 2H), 5.17 (s, 1H), 3.72 (s, 3H), 3.41 (dd, J = 9.5, 4.7 Hz, 1H), 3.05 (q, J = 6.6 Hz, 2H), 2.94 (dd, J = 15.2, 4.6 Hz, 1H), 2.70 (dd, J = 15.2, 9.5 Hz, 1H), 1.93 (t, J = 7.4 Hz, 2H), 1.48 (p, J = 7.4 Hz, 2H), 1.39 (p, J = 7.4 Hz, 2H), 1.30–1.19 (m, 2H). ^{13}C NMR (101 MHz, DMSO-d$_6$) δ: 172.56, 169.07, 158.38, 136.04, 134.99, 134.97, 134.75, 129.41, 126.71, 118.28, 117.61, 113.45, 110.99, 107.78, 55.09, 53.33, 51.68, 38.35, 32.23, 28.87, 26.04, 25.19, 24.89. $[\alpha]_D^{20}$ = 42.66 (0.10 mg mL^{-1}, MeOH). ESI-MS m/z: 450.5 [M + H]$^+$.

5.1.3.12 (1S,3R)-N-(7-(Hydroxyamino)-7-oxoheptyl)-1-(4-methoxyphenyl)-2,3,4,9-tetrahydro-1H-pyrido[3,4-b]indole-3-carboxamide (13c). White solid, yield of 48.3%, m.p.: 104.2–106.4 °C. ^{1}H NMR (400 MHz, DMSO-d$_6$) δ: 10.71 (s, 1H), 10.34 (s, 1H), 8.67 (s, 1H), 7.82 (t, J = 5.6 Hz, 1H), 7.44 (d, J = 7.7 Hz, 1H), 7.25 (d, J = 7.7 Hz, 1H), 7.13 (d, J = 8.6 Hz, 2H), 7.03 (t, J = 7.4 Hz, 1H), 6.96 (t, J = 7.4 Hz, 1H), 6.88 (d, J = 8.6 Hz, 2H), 5.17

(s, 1H), 3.72 (s, 3H), 3.41 (dd, J = 9.5, 4.9 Hz, 1H), 3.04 (dt, J = 10.9, 5.8 Hz, 2H), 2.94 (dd, J = 15.1, 4.7 Hz, 1H), 2.70 (dd, J = 15.1, 9.3 Hz, 1H), 1.93 (t, J = 7.4 Hz, 2H), 1.52–1.43 (m, 2H), 1.43–1.34 (m, 2H), 1.28–1.20 (m, 4H). ^{13}C NMR (101 MHz, DMSO-d$_6$) δ: 172.56, 169.11, 158.38, 136.03, 134.99, 134.76, 129.40, 126.71, 120.75, 118.28, 117.60, 113.44, 110.98, 107.76, 55.09, 53.31, 51.70, 38.38, 32.25, 29.00, 28.31, 26.13, 25.16, 25.10. $[\alpha]_D^{20}$ = 43.20 (0.09 mg mL^{-1}, MeOH). ESI-MS m/z: 465.6 [M + H]$^+$.

5.1.3.13 (1S,3R)-1-Cyclopropyl-N-(7-(hydroxyamino)-7-oxoheptyl)-2-(4-methoxybenzyl)-2,3,4,9-tetrahydro-1H-pyrido[3,4-b]indole-3-carboxamide (13d). White solid, yield of 52.1%, m.p.: 113.2–115.6 °C. ^{1}H NMR (400 MHz, DMSO-d$_6$) δ: 10.53 (s, 1H), 10.31 (s, 1H), 8.64 (s, 1H), 7.87–7.66 (m, 1H), 7.45 (d, J = 7.6 Hz, 1H), 7.33–7.23 (m, 3H), 7.07–6.93 (m, 2H), 6.87 (d, J = 7.2 Hz, 2H), 4.17–4.01 (m, 1H), 3.74 (s, 3H), 3.63–3.58 (m, 1H), 3.04–2.96 (m, 1H), 2.91–2.78 (m, 2H), 2.71 (dd, J = 14.1, 3.7 Hz, 1H), 1.93–1.82 (m, 2H), 1.46–1.33 (m, 4H), 1.29–1.11 (m, 4H), 0.54–0.41 (m, 2H), 0.39–0.31 (m, 1H), 0.17–0.07 (m, 1H). ^{13}C NMR (101 MHz, DMSO-d$_6$) δ: 171.65, 169.12, 158.33, 138.83, 136.15, 129.37, 126.48, 120.68, 117.73, 113.65, 111.30, 111.01, 110.11, 88.26, 65.44, 55.04, 38.47, 32.23, 29.31, 28.35, 28.34, 26.15, 25.08, 15.58, 3.47. $[\alpha]_D^{20}$ = −17.20 (0.05 mg mL^{-1}, MeOH). ESI-MS m/z: 519.7 [M + H]$^+$.

5.1.3.14 (1S,3R)-N-(6-(Hydroxyamino)-6-oxohexyl)-2-(4-methoxybenzyl)-1-methyl-2,3,4,9-tetrahydro-1H-pyrido[3,4-b]indole-3-carboxamide (13e). Yellow solid, yield of 47.5%, m.p.: 92.4–94.1 °C. ^{1}H NMR (400 MHz, DMSO-d$_6$) δ: 10.63 (s, 1H), 10.30 (s, 1H), 8.65 (s, 1H), 7.86 (t, J = 5.9 Hz, 1H), 7.43 (d, J = 7.9 Hz, 1H), 7.32 (d, J = 8.5 Hz, 2H), 7.25 (d, J = 7.9 Hz, 1H), 7.02 (t, J = 7.4 Hz, 1H), 6.96 (t, J = 7.4 Hz, 1H), 6.88 (d, J = 8.5 Hz, 2H), 3.87 (dd, J = 10.4, 4.9 Hz, 1H), 3.81–3.76 (m, 1H), 3.74 (s, 3H), 3.58 (d, J = 14.0 Hz, 1H), 3.01 (dd, J = 12.7, 6.9 Hz, 1H), 2.93–2.83 (m, 1H), 2.76 (dd, J = 16.7, 5.2 Hz, 1H), 1.85 (t, J = 7.4 Hz, 2H), 1.46–1.37 (m, 6H), 1.24–1.14 (m, 3H). ^{13}C NMR (101 MHz, DMSO-d$_6$) δ: 171.65, 169.01, 158.25, 136.13, 136.00, 131.15, 129.15, 126.84, 120.49, 118.28, 117.64, 113.69, 110.82, 105.25, 56.25, 55.01, 51.07, 50.28, 38.34, 32.16, 29.09, 26.00, 24.84, 20.74, 18.76. $[\alpha]_D^{20}$ = −88.39 (0.05 mg mL^{-1}, MeOH). ESI-MS m/z: 478.6 [M + H]$^+$.

5.1.3.15 (1S,3R)-N-(7-(Hydroxyamino)-7-oxoheptyl)-2-(4-methoxybenzyl)-1-methyl-2,3,4,9-tetrahydro-1H-pyrido[3,4-b]indole-3-carboxamide (13f). White solid, yield of 47.5%, m.p.: 97.6–99.5 °C. ^{1}H NMR (400 MHz, DMSO-d$_6$) δ: 10.63 (s, 1H), 10.30 (s, 1H), 8.63 (s, 1H), 7.85 (t, J = 5.8 Hz, 1H), 7.43 (d, J = 7.9 Hz, 1H), 7.32 (d, J = 8.4 Hz, 2H), 7.25 (d, J = 7.9 Hz, 1H), 7.02 (t, J = 7.4 Hz, 1H), 6.96 (t, J = 7.3 Hz, 1H), 6.88 (d, J = 8.6 Hz, 2H), 3.87 (dd, J = 10.5, 4.8 Hz, 1H), 3.83–3.75 (m, 2H), 3.74 (s, 3H), 3.59 (d, J = 14.0 Hz, 1H), 3.44–3.37 (m, 2H), 3.01 (m, 1H), 2.92–2.84 (m, 1H), 2.80–2.72 (m, 1H), 1.87 (t, J = 7.3 Hz, 2H), 1.39 (d, J = 6.7 Hz, 4H), 1.23 (m, 2H), 1.21–1.17 (m, 3H). ^{13}C NMR (101 MHz, DMSO-d$_6$) δ: 171.69, 169.10, 158.28, 136.16, 136.02, 131.15, 129.14, 126.86, 120.53, 118.31, 117.67, 113.70, 110.85, 105.27, 56.27, 55.03, 51.09, 50.33, 38.40, 32.22, 29.26, 28.34, 26.12, 25.05, 20.78, 18.78. $[\alpha]_D^{20}$ = −48.30 (0.05 mg mL^{-1}, MeOH). ESI-MS m/z: 493.6 [M + H]$^+$.

5.1.3.16 (1S,3R)-2-Benzyl-1-cyclopropyl-N-(7-(hydroxyamino)-7-oxoheptyl)-2,3,4,9-tetrahydro-1H-pyrido[3,4-b]indole-3-carboxamide (13g). White solid, yield of 48.3%, m.p.: 103.6–105.3 °C. ^{1}H NMR (400 MHz, DMSO-d$_6$) δ: 10.54 (s, 1H), 10.32 (s, 1H), 8.66 (s, 1H), 7.87–7.75 (m, 1H), 7.46 (d, J = 7.7 Hz, 1H), 7.40 (d, J = 7.4 Hz, 2H), 7.34–7.20 (m, 4H), 7.04 (t, J = 7.4 Hz, 1H), 6.97 (t, J = 7.4 Hz, 1H), 4.12 (dd, J = 10.6, 5.3 Hz, 1H), 3.70 (d, J = 14.2 Hz, 1H), 3.35–3.28 (m, 2H), 3.10–3.03 (m, 1H), 3.01 (d, J = 7.7 Hz, 1H), 2.97–2.79 (m, 2H), 1.86 (t, J = 7.4 Hz, 2H), 1.46–1.31 (m, 4H), 1.27–1.09 (m, 4H), 0.54–0.43 (m, 2H), 0.43–0.29 (m, 1H), 0.24–0.10 (m, 1H). ^{13}C NMR (101 MHz, DMSO-d$_6$) δ: 171.60, 169.13, 139.32, 136.16, 133.72, 128.26, 128.17, 126.99, 126.69, 120.71, 118.37, 117.76, 111.03, 106.03, 59.31, 57.14, 51.47, 38.49, 32.25, 29.31, 28.37, 26.16, 25.08, 18.72, 15.61, 3.53, 3.45. $[\alpha]_D^{20}$ = 19.67 (0.06 mg mL^{-1}, MeOH). ESI-MS m/z: 489.6 [M + H]$^+$.

5.1.3.17 (1S,3R)-1-(4-Chlorophenyl)-N-(6-(hydroxyamino)-6-oxohexyl)-2,3,4,9-tetrahydro-1H-pyrido[3,4-b]indole-3-carboxamide (13h). White solid, yield of 55.4%, m.p.: 117.6–119.8 °C. ^{1}H NMR (400 MHz, DMSO-d$_6$) δ: 10.75 (s, 1H), 10.33 (s, 1H), 8.66 (s, 1H), 7.83 (t, J = 5.7 Hz, 1H), 7.45 (d, J = 7.7 Hz, 1H), 7.38 (d, J = 8.5 Hz, 2H), 7.29–7.21 (m, 3H), 7.04 (t, J = 7.5 Hz, 1H), 6.97 (t, J = 7.4 Hz, 1H), 5.21 (s, 1H), 3.04 (q, J = 6.7 Hz, 2H), 2.92 (dd, J = 15.3, 4.7 Hz, 1H), 2.70 (dd, J = 15.3, 9.6 Hz, 1H), 1.92 (t, J = 7.4 Hz, 2H), 1.47 (p, J = 7.5 Hz, 2H), 1.39 (p, J = 7.2 Hz, 2H), 1.29–1.18 (m, 2H). ^{13}C NMR (101 MHz, DMSO-d$_6$) δ: 172.45, 169.07, 142.03, 136.06, 133.96, 131.61, 128.02, 126.67, 120.94, 118.39, 117.71, 111.05, 108.04, 53.16, 51.75, 38.35, 32.22, 28.84, 26.03, 25.16, 24.88. $[\alpha]_D^{20}$ = 52.78 (0.11 mg mL^{-1}, MeOH). ESI-MS m/z: 454.9 [M + H]$^+$.

5.1.3.18 (1S,3R)-1-(4-Chlorophenyl)-N-(7-(hydroxyamino)-7-oxoheptyl)-2,3,4,9-tetrahydro-1H-pyrido[3,4-b]indole-3-carboxamide (13i). White solid, yield of 39.6%, m.p.: 99.8–101.4 °C. ^{1}H NMR (400 MHz, DMSO-d$_6$) δ: 10.76 (s, 1H), 10.34 (s, 1H), 8.67 (s, 1H), 7.83 (t, J = 5.7 Hz, 1H), 7.45 (d, J = 7.7 Hz, 1H), 7.38 (d, J = 8.4 Hz, 2H), 7.30–7.22 (m, 3H), 7.05 (t, J = 7.1 Hz, 1H), 6.97 (t, J = 7.1 Hz, 1H), 5.22 (s, 1H), 3.41–3.36 (m, 1H), 3.05 (q, J = 6.7 Hz, 2H), 2.93 (dd, J = 15.2, 4.7 Hz, 1H), 2.71 (dd, J = 15.2, 9.5 Hz, 1H), 1.93 (t, J = 7.2 Hz, 2H), 1.48 (q, J = 7.2 Hz, 2H), 1.38 (q, J = 6.9 Hz, 2H), 1.29–1.20 (m, 4H). ^{13}C NMR (101 MHz, DMSO-d$_6$) δ: 172.47, 169.12, 142.06, 136.08, 134.00, 131.63, 130.14, 128.03, 126.69, 120.95, 118.40, 117.72, 111.07, 108.05, 53.17, 51.79, 38.41, 32.26, 29.00, 28.33, 26.14, 25.17, 25.11. $[\alpha]_D^{20}$ = 41.60 (0.10 mg mL^{-1}, MeOH). ESI-MS m/z: 468.9 [M + H]$^+$.

5.1.3.19 (1S,3R)-1-(3,4-Dimethoxyphenyl)-N-(7-(hydroxyamino)-7-oxoheptyl)-2,3,4,9-tetrahydro-1H-pyrido[3,4-b]indole-3-carboxamide (13j). White solid, yield of 42.8%, m.p.: 113.1–116.7 °C. ^{1}H NMR (400 MHz, DMSO-d$_6$) δ: 10.72 (s, 1H), 10.34 (s, 1H), 8.67 (s, 1H), 7.86 (t, J = 5.5 Hz, 1H), 7.44 (d, J = 7.7 Hz, 1H), 7.25 (d, J = 8.0 Hz, 1H), 7.06–6.93 (m, 3H), 6.85 (d, J = 8.3 Hz, 1H), 6.57 (d, J = 8.3 Hz, 1H), 5.16 (s, 1H), 3.72 (s, 3H), 3.71 (s, 3H), 3.45 (dd, J = 9.3, 4.7 Hz, 1H), 3.06 (q, J = 6.6 Hz, 2H), 2.94 (dd, J = 15.2, 4.7 Hz, 1H), 2.77–2.65 (m, 1H), 1.93 (t, J = 7.3 Hz, 2H), 1.50–1.37 (m, 4H), 1.25–1.20 (m, 4H). ^{13}C NMR (101 MHz, DMSO-d$_6$) δ: 172.60, 169.15, 148.67, 148.05, 136.06, 126.71, 120.79, 120.23, 118.30, 117.65, 112.31, 111.24, 111.02, 107.73, 55.59, 55.53, 53.66, 51.90, 38.39, 32.27, 29.05, 28.34, 26.16, 25.12. $[\alpha]_D^{20}$ = 42.0 (0.07 mg mL^{-1}, MeOH). ESI-MS m/z: 494.6 [M + H]$^+$.

5.2 *In vitro* HDAC enzyme assay

IC_{50} testing of compounds was performed by Reaction Biology Corporation. The HDACs were isolated from a baculovirus expression system in Sf9 cells using an acetylated fluorogenic peptide, $RHKK_{Ac}$, as the substrate. The reaction buffer was made up of 50 mM Tris–HCl pH 8.0, 127 mM NaCl, 2.7 mM KCl, 1 mM $MgCl_2$, 1 mg per mL BSA, and a final concentration of 1% DMSO. Compounds were delivered in DMSO and delivered to an enzyme mixture with a preincubation of 5–10 min followed by substrate addition and incubation for 2 h at 30 °C. Trichostatin A and a developer were added to quench the reaction and generate fluorescence, respectively. Dose–response curves were generated starting at 30 μM of compound with 3-fold serial dilutions to generate a 10-dose plot. IC_{50} values were then generated from the resulting plots. The detailed protocol can be found in ref. 25.

5.3 Cell culture and cell viability assay

The cells were cultured in IMDM medium with 20% FBS, 100 U per mL penicillin and 100 μg per mL streptomycin. Briefly, a 100 μL cell suspension or completed medium were plated into a 96-well plate. Compounds were added and incubated for 72 h. Subsequently, 22 μL Alamar blue solution (1 mM) was pipetted into each well of the 96-well plate; and the plates were incubated for an additional 5–6 h. The absorbance (OD) was read at 530/590 nm. Data were normalized to vehicle groups and represented as the means of three independent measurements with standard errors of <20%. The IC_{50} values were calculated using Prism 5.0.

For NCI-60 screening, all details of the test method are described on the NCI Web site (https://dtp.cancer.gov/discovery_development/nci-60/methodology.htm).

5.4 Computational methods

Sybyl-X 2.0 software (Saint Louis, MO, USA) was used for simulation. Docking was conducted based on the cocrystal of HDAC1 (PDB: 5ICN). HDAC1 was used as the receptor. The cavity occupied by a polypeptide was selected as binding site. Water molecules outside the binding pocket were excluded. The other docking parameters were kept as default.

Conflicts of interest

The authors declare that they have no known competing financial interests or personal relationships that could have appeared to influence the work reported in this paper.

Acknowledgements

References

1 M. Shirvaliloo, *Epigenomics*, 2022, **14**, 1465–1477.
2 Y. Zhang, Z. Sun, J. Jia, T. Du, N. Zhang, Y. Tang, Y. Fang and D. Fang, *Adv. Exp. Med. Biol.*, 2021, **1283**, 1–16.
3 R. Sarkar, S. Banerjee, S. A. Amin, N. Adhikari and T. Jha, *Eur. J. Med. Chem.*, 2020, **192**, 112171.
4 A. Badie, C. Gaiddon and G. Mellitzer, *Cancers*, 2022, **14**, 5472.
5 E. Shirbhate, R. Veerasamy, S. H. S. Boddu, A. K. Tiwari and H. Rajak, *Drug Discovery Today*, 2022, **27**, 1689–1697.
6 A. J. de Ruijter, A. H. van Gennip, H. N. Caron, S. Kemp and A. B. van Kuilenburg, *Biochem. J.*, 2003, **370**, 737–749.
7 I. V. Gregoretti, Y. M. Lee and H. V. Goodson, *J. Mol. Biol.*, 2004, **338**, 17–31.
8 G. P. Delcuve, D. H. Khan and J. R. Davie, *Expert Opin. Ther. Targets*, 2013, **17**, 29–41.
9 P. A. Marks and R. Breslow, *Nat. Biotechnol.*, 2007, **25**, 84–90.
10 A. Sawas, D. Radeski and O. A. O'Connor, *Ther. Adv. Hematol.*, 2015, **6**, 202–208.
11 J. P. Laubach, P. Moreau, J. F. San-Miguel and P. G. Richardson, *Clin. Cancer Res.*, 2015, **21**, 4767–4773.
12 S. A. Reddy, *Crit. Rev. Oncol./Hematol.*, 2016, **106**, 99–107.
13 M. Dong, Z. Q. Ning, P. Y. Xing, J. L. Xu, H. X. Cao, G. F. Dou, Z. Y. Meng, Y. K. Shi, X. P. Lu and F. Y. Feng, *Cancer Chemother. Pharmacol.*, 2012, **69**, 1413–1422.
14 Z. Q. Ning, Z. B. Li, M. J. Newman, S. Shan, X. H. Wang, D. S. Pan, J. Zhang, M. Dong, X. Du and X. P. Lu, *Cancer Chemother. Pharmacol.*, 2012, **69**, 901–909.
15 T. Liang, F. Wang, R. M. Elhassan, Y. Cheng, X. Tang, W. Cheng, H. Fang and X. Hou, *Acta Pharm. Sin. B*, 2023, **13**, 2425–2463.
16 T. Liang, Z. Xie, B. Dang, J. Wang, T. Zhang, X. Luan, T. Lu, C. Cao and X. Chen, *Bioorg. Med. Chem. Lett.*, 2023, **81**, 129148.
17 T. C. S. Ho, A. H. Y. Chan and A. Ganesan, *J. Med. Chem.*, 2020, **63**, 12460–12484.
18 X. Chen, S. Zhao, H. Li, X. Wang, A. Geng, H. Cui, T. Lu, Y. Chen and Y. Zhu, *Eur. J. Med. Chem.*, 2019, **168**, 110–122.
19 X. Chen, X. Chen, R. R. Steimbach, T. Wu, H. Li, W. Dan, P. Shi, C. Cao, D. Li, A. K. Miller, Z. Qiu, J. Gao and Y. Zhu, *Eur. J. Med. Chem.*, 2020, **187**, 111950.
20 X. Chen, G. Gong, X. Chen, R. Song, M. Duan, R. Qiao, Y. Jiao, J. Qi, Y. Chen and Y. Zhu, *Chem. Pharm. Bull.*, 2019, **67**, 1116–1122.
21 G. Gong, J. Qi, Y. Lv, S. Dong, C. Cao, D. Li, R. Zhao, Z. Li and X. Chen, *Chem. Pharm. Bull.*, 2020, **68**, 466–472.
22 L. Santo, T. Hideshima, A. L. Kung, J. C. Tseng, D. Tamang, M. Yang, M. Jarpe, J. H. van Duzer, R. Mazitschek, W. C. Ogier, D. Cirstea, S. Rodig, H. Eda, T. Scullen, M. Canavese, J. Bradner, K. C. Anderson, S. S. Jones and N. Raje, *Blood*, 2012, **119**, 2579–2589.
23 N. Arrighetti, C. Corno and L. Gatti, *Crit. Rev. Oncog.*, 2015, **20**, 83–117.
24 J. Wang, F. Gong, T. Liang, Z. Xie, Y. Yang, C. Cao, J. Gao, T. Lu and X. Chen, *Eur. J. Med. Chem.*, 2021, **225**, 113815.

25 X. Chen, J. Wang, P. Zhao, B. Dang, T. Liang, R. R. Steimbach, A. K. Miller, J. Liu, X. Wang, T. Zhang, X. Luan, J. Hu and J. Gao, *Eur. J. Med. Chem.*, 2023, **260**, 115776.

26 W. Wen, J. Hu, C. Wang, R. Yang, Y. Zhang, B. Huang, T. Qiao, J. Wang and X. Chen, *Bioorg. Med. Chem. Lett.*, 2024, 129670, DOI: **10.1016/j.bmcl.2024.129670**.

27 S. Khochbin, A. Verdel, C. Lemercier and D. Seigneurin-Berny, *Curr. Opin. Genet. Dev.*, 2001, **11**, 162–166.